

Proteomics-based Target Identification

BENGAMIDES AS A NEW CLASS OF METHIONINE AMINOPEPTIDASE INHIBITORS*

Received for publication, August 14, 2003, and in revised form, October 2, 2003
Published, JBC Papers in Press, October 8, 2003, DOI 10.1074/jbc.M309039200

Harry Towbin^{‡§}, Kenneth W. Bair[¶], James A. DeCaprio^{**}, Michael J. Eck^{**}, Sunkyu Kim[¶],
Frederick R. Kinder[¶], Anthony Morollo^{**}, Dieter R. Mueller[‡], Patrick Schindler[‡],
Hyun Kyu Song^{**}, Jan van Oostrum[‡], Richard W. Versace[¶], Hans Voshol[‡], Jeanette Wood[‡],
Sonya Zabludoff^{¶‡‡}, and Penny E. Phillips^{¶§§}

From [‡]Novartis Pharma AG, CH-4036 Basle, Switzerland, [¶]Novartis Pharmaceuticals, East Hanover, New Jersey 07936, and ^{**}Department of Cancer Biology, Dana-Farber Cancer Institute, and Department of Biological Chemistry and Molecular Pharmacology, Harvard Medical School, Boston, Massachusetts 02115

LAF389 is a synthetic analogue of bengamides, a class of marine natural products that produce inhibitory effects on tumor growth *in vitro* and *in vivo*. A proteomics-based approach has been used to identify signaling pathways affected by bengamides. LAF389 treatment of cells resulted in altered mobility of a subset of proteins on two-dimensional gel electrophoresis. Detailed analysis of one of the proteins, 14-3-3 γ , showed that bengamide treatment resulted in retention of the amino-terminal methionine, suggesting that bengamides directly or indirectly inhibited methionine aminopeptidases (MetAps). Both known MetAps are inhibited by LAF389. Short interfering RNA suppression of MetAp2 also altered amino-terminal processing of 14-3-3 γ . A high resolution structure of human MetAp2 co-crystallized with a bengamide shows that the compound binds in a manner that mimics peptide substrates. Additionally, the structure reveals that three key hydroxyl groups on the inhibitor coordinate the di-cobalt center in the enzyme active site.

Bengamides are natural products originally isolated from marine sponges (1). Bengamide B is one of the most potent members of the family; it causes growth inhibition *in vitro* at low nM concentrations on all human tumor cell lines tested (2). *In vivo*, it significantly inhibits growth of MDA-MB435 human breast cancer xenografts at well tolerated doses (3). *In vitro* studies of bengamide B suggested its activity might be due to inhibition of a novel target, because its pattern of activity in the NCI 60 cell line screening panel was unique compared with that of other chemotherapeutic agents (2). Although bengamide

B was a potent lead structure, its limited availability from natural sources, the complexity of its synthesis, and its relatively poor solubility prevented further development of the compound as a therapeutic agent. Therefore, a synthetic chemistry program was initiated to develop analogues of bengamide B with enhanced solubility and ease of synthesis. LAF389 was selected from a number of analogues because of its equivalent activity *in vitro* against a broad panel of human tumor cell lines and its improved activity in human tumor xenograft models (3).

As was the case with bengamide B, the profile of LAF389 in standard cytotoxicity assays and tests of its effects on conventional cytotoxic targets did not suggest the molecular target of the compound. Because such knowledge can help to develop more potent or selective inhibitors and is also helpful in selecting the most responsive tumor types for clinical use, a number of approaches were used to determine a molecular target. LAF389 was not active in assays for DNA binding and damage, topoisomerase binding, polymerization of microtubules and actin, or proteasome function (data not shown). Similarly, no changes in mRNA transcription were detected in studies on transcriptional effects where cells were challenged for 8 h with LAF389. The relatively short exposure time was chosen to narrow the responses to initial effects on or close to the affected target.

Here, we report on the identification of a molecular target for bengamides based on proteomic studies performed on cells treated *in vitro* with LAF389. Proteomics approaches have the potential to discover effects at the level of posttranslational modifications of proteins, an area where other powerful techniques such as RNA profiling experiments are not directly informative. In this case, proteomic analysis has proven pivotal to the discovery of methionine aminopeptidases as a molecular target for bengamides.

EXPERIMENTAL PROCEDURES

Cloning, Expression, and Assay of Human Methionine Aminopeptidases—Human MetAp 1 and 2 were PCR-amplified based on published sequences (4–6), expressed as N-terminal glutathione S-transferase-tagged proteins in insect cells, and purified over GSH columns. Enzyme assays were run using MetAp enzyme (5.2 μ g/ml, 100 nM) incubated with Met-Ala-Ser tripeptide substrate (Bachem; 1 mM) and inhibitor compounds in 66 μ l of assay buffer for 1 h at room temperature. Assay buffer was 50 mM KH₂PO₄, pH 7.5, 0.4 mM CoCl₂, 0.02% bovine serum albumin. Reactions were terminated, and released methionine was visualized by the addition of 80 μ l of ninhydrin solution (30 mM ninhydrin, 30 mM CdCl₂, 12.2% acetic acid). Plates were incubated 1 h at room temperature and read at 490 nm.

Purification and Synthesis of Bengamide Analogues—The syntheses of bengamide E, LAF153, and LAF389 have been reported previously (3, 7). Structures of the compounds are given in Fig. 1.

* The costs of publication of this article were defrayed in part by the payment of page charges. This article must therefore be hereby marked "advertisement" in accordance with 18 U.S.C. Section 1734 solely to indicate this fact.

The atomic coordinates and structure factors (code 1QZY) have been deposited in the Protein Data Bank, Research Collaboratory for Structural Bioinformatics, Rutgers University, New Brunswick, NJ (<http://www.rcsb.org/>).

§ To whom correspondence should be addressed: Novartis Pharma AG, Lichstrasse 35, CH-4036 Basle, Switzerland. Tel.: 4161-324-4331; Fax: 4161-324-9860; E-mail: harry.towbin@pharma.novartis.com.

¶ Present address: Chiron Corporation, 4560 Horton St. MS4.6126, Emeryville, CA 94608-2916.

‡‡ Present address: AstraZeneca Corporation, 35 Gatehouse Drive, Waltham, MA 02451.

§§ To whom correspondence should be addressed: Novartis Pharmaceuticals, One Health Plaza, East Hanover, NJ 07936. Tel.: 862-778-0097; Fax: 973-781-8265; E-mail: penny.phillips@pharma.novartis.com.

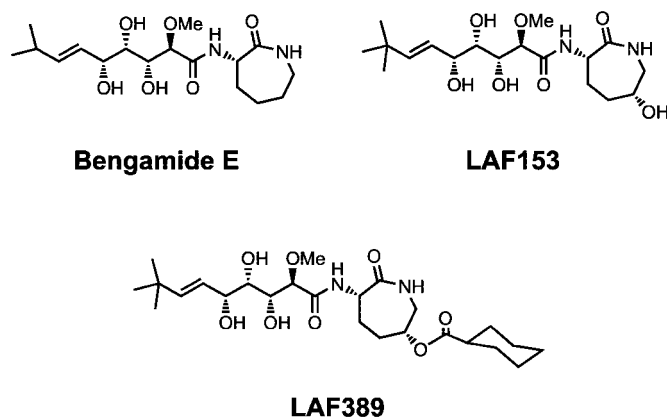


FIG. 1. Structures of bengamide E, LAF389, and LAF153.

Cell Culture and Proliferation Assays—H1299 human small cell lung carcinoma and A549 human non-small cell lung carcinoma cells were cultivated in RPMI 1640 medium supplemented with 10% fetal calf serum and glutamine. Human umbilical vein endothelial cells (HUVEC)¹ were purchased from Clonetics and cultured according to the manufacturer's protocol. All maintenance media contained 100 units/ml penicillin and 100 μ g/ml streptomycin. Antiproliferative effects of LAF389 *in vitro* were measured as described previously (3).

IEF Sample Preparation and Immunoblotting—Cell samples were washed with phosphate-buffered saline and the cell pellet was dissolved in a buffer containing 4% CHAPS, 7 M urea, 2 M thiourea, 10 mg/ml dithiothreitol, and 1% pharmalytes (pH 3–10) (8). Isoelectric focusing of samples and transfer to membranes was performed as described (9).

Two-dimensional Electrophoresis and Proteomics Techniques—The methodology described earlier (10) was used. For resolving the 14-3-3 isoforms, ultrazoom pH gradient strips in the range of pH 4.5–5.5 (Amersham Pharmacia Biotech, Uppsala, Sweden) were used.

Western Blots—Rabbit polyclonal antibodies against 14-3-3 proteins (pan-reactive and isotype-specific) were obtained from Santa Cruz Biotechnology (Santa Cruz, CA). A monoclonal antibody specific to the amino terminus of 14-3-3 γ was raised against a peptide corresponding to the N-terminal 15 amino acid residues, beginning with methionine, coupled to keyhole limpet hemocyanin. Specificity of the antibody was confirmed by testing against both the immunizing peptide as well as a 15-mer peptide missing the initial methionine and beginning with an acetylated valine (data not shown).

siRNA—MetAp2 suppression was performed using an siRNA sequence designed as described (11). The targeting sequence was AAUGCCGUGACACAACAUGA (Dharmacon Research). The control mismatch sequence was AAUGCCGGCGCUACAACAUGA. Duplex RNA was introduced into H1299 cells using LipofectAMINE 2000 (Invitrogen) according to the manufacturer's protocol. Duplex RNA was introduced into HUVECs by electroporation.

Structure Determination—The full-length human methionine aminopeptidase-2 protein was expressed by using a baculovirus/insect cell system and was purified as described previously (12). Crystals isomorphous to the previously described unliganded and fumagillin-bound MetAp2 (13) were obtained by vapor diffusion at 4 °C by combining 2 μ l of MetAp2 protein in storage buffer (10 mM Hepes, pH 7.0, 150 mM NaCl, 1 mM CoCl₂, and 10% glycerol) with 2 μ l of a reservoir solution containing 30% *t*-butyl alcohol and 50 mM sodium citrate, pH 5.5. For co-crystallization with LAF153, an approximately 4-fold molar excess of the inhibitor was added to the protein solution (in ethanol). Diffraction data were recorded at 100 K on the A1 station at the Cornell High Energy Synchrotron Source and processed using DENZO and SCALEPACK (13). The structure was determined by rigid body refinement of the unliganded MetAp2 structure (Protein Data Bank code 1BN5) against the LAF153 data set. The structure and inhibitor was fit to the electron density with the program O (14). Crystallographic refinement

TABLE I

Proteins with altered mobility in two-dimensional gel electrophoresis after treatment of H1299 cells with 25 μ M bengamide E for 8 h

Protein name	Change
PP2A inhibitor	42 kDa, pI 4.0 in control, pI 4.4 in treated
Nucleophosmin B23	39 kDa, pI 4.8 in control, pI 5.3 in treated
Methionine aminopeptidase 2	80 kDa, pI 5.7 in control, pI 5.5 in treated
L protein	75 kDa, pI 7.8 in control, pI 7.7 in treated
67 kDa laminin receptor	36 kDa, pI 4.4 intensity up in control
Triosephosphate isomerase	30 kDa, pI 7.2 intensity up in treated
eIF2 α	40 kDa, pI 4.8 in control, pI 5.0 in treated
EB1	35 kDa, pI 5.0 intensity up in treated
14-3-3 isoforms	30 kDa, pI 4.5 in control, pI 4.6 in treated

with the program CNS (15) yielded a final R value of 20.4% ($R_{\text{free}} = 21.1\%$) using all data to 1.6 Å resolution. Crystallographic data collection and refinement statistics are presented in Table II. Coordinates for the x-ray structure of the MetAp2/LAF153 complex have been deposited with the Protein Data Bank under code 1QZY.

RESULTS

A Proteomics Approach Identifies an Alteration in a 14-3-3 Protein after LAF389 Treatment—A pilot study was performed using two-dimensional electrophoresis to analyze differences in protein expression of H1299 cells after treatment with a natural bengamide, bengamide E. In the initial experiments, roughly 1500 protein spots were visualized, and a limited number of differences were observed after bengamide treatment. Protein spots that were reproducibly altered in intensity were identified using MALDI-MS. Determination of tryptic peptide masses permitted identification of the parent protein in most cases (Table I). Examination of the differentially expressed proteins did not immediately suggest a common pathway affected by bengamide treatment, because with the exception of MetAp2 and eIF2 α , the proteins are not known to be associated or co-regulated. One feature of the identified proteins was that a subset had treatment-dependent changes in charge, rather than changes in mass or abundance. Such changes are likely to arise from post-translational modifications, including phosphorylation and acetylation. A notable protein included in this set was a member of the 14-3-3 protein family. 14-3-3 proteins are ubiquitous cytosolic adaptor proteins that bind to specific phosphoserine-containing motifs and modulate intracellular signaling, cell cycle control, transcriptional control, and apoptosis (16). In humans, seven isoforms are encoded by a multigene family. Several isoforms are post-translationally modified by phosphorylation (17, 18) and N-terminal acetylation (19).

Further analysis of the altered 14-3-3 proteins was pursued by using cells treated with the synthetic bengamide LAF389. Initial experiments with two-dimensional gel electrophoresis confirmed that LAF389 treatment of H1299 cells shifted the isoelectric point of a 14-3-3 isoform, similar to the effects seen in pilot experiments using bengamide E (Fig. 2A). To broaden the observation of bengamide effects on changes in 14-3-3 isoforms and characterize which of the closely related 14-3-3 isoforms were altered by bengamide treatment, an analytical blotting method was used that resolved 14-3-3 isoforms by isoelectric focusing of cell lysates, followed by Western blotting using antibodies to 14-3-3 proteins (9). In experiments not shown, we studied the kinetics and LAF389 concentration dependence of the appearance of the base-shifted 14-3-3 protein.

¹ The abbreviations used are: HUVEC, human umbilical vein endothelial cells; CHAPS, 3-(3-cholamidopropyl)dimethylammonium-1-propanesulfonic acid; siRNA, short interfering RNA; IEF, immuno-electrophoresis; MALDI-MS, matrix-assisted laser desorption/ionization mass spectrometry; ESMS/MS, electrospray tandem mass spectrometry; MetAps, methionine aminopeptidases.

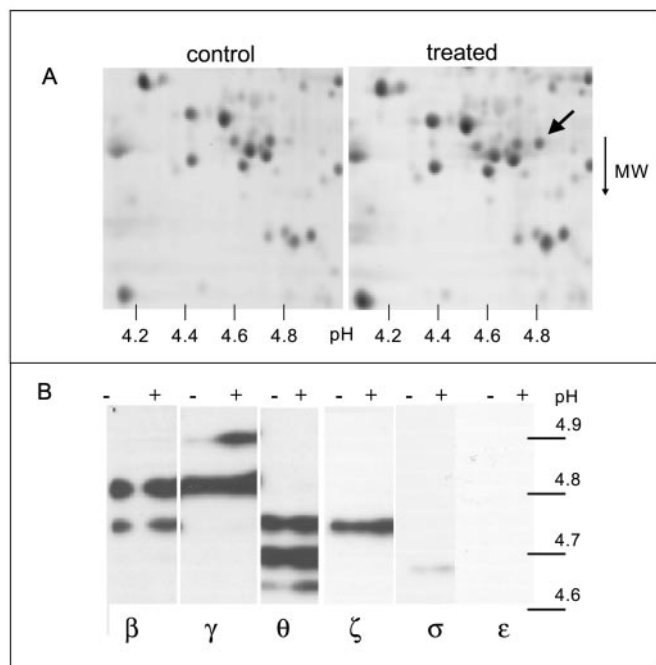


FIG. 2. LAF389 treatment of cells causes changes in mobility of a 14-3-3 isoform. Lysates were prepared from H1299 cells treated with LAF389 (200 nM, 24 h) or vehicle control. *A*, sections of representative two-dimensional electrophoresis gels (pH 4–7) of control (*left*) and LAF389-treated (*right*) samples. *Arrow* indicates 14-3-3 spot selected for further processing. *B*, lysates of control (–) and LAF389-treated (+) cells were resolved by IEF-immunoblotting (pH 4.5–5.4) and probed for 14-3-3 reactivity by using antibodies specific for the β , γ , θ , ζ , σ , and ϵ isoforms. The reaction with the anti- σ antibody was weak; no reaction was detected with an anti- ϵ antibody.

The band became detectable after about 8 h and accumulated for 48 h. After 24 h of incubation, effects in H1299 cells were observed at 3 nM LAF389, with gradual increases up to 300 nM, the highest concentration tested. The bengamide-responsive 14-3-3 isoform was then identified by testing cell lysates from LAF389-treated and control H1299 cells with the IEF immunoblotting method. The immunoblots were probed in parallel samples with isoform-specific polyclonal antibodies (Fig. 2*B*). Only the 14-3-3 γ specific antibody recognized the inducible and more basic band, consistent with the shift seen in the original two-dimensional gels. The observed pH shift of 0.07 pH units was compatible with the theoretically calculated shift of 0.06 for a loss of one negative charge. For the generality of the response, three cell lines (U2OS, MDA-MB-435, and A549) were analyzed by this method, now using the γ -specific antibody. In all cell lines, LAF389 induced the base-shifted form of 14-3-3 γ (data not shown).

To corroborate these findings, extracts of LAF389-treated H1299 cells as well as control cells were separated by two-dimensional electrophoresis, where the first dimension was on a zoom gel (pH 4.5–5.5 over a distance of 18 cm). The region of the 14-3-3 proteins was identified from a contact blot of the two-dimensional gel that was probed with a pan-isoform-reactive anti-14-3-3 antibody. A series of proteins in the antibody-reactive region, including the additional isoform, was cut from a silver-stained two-dimensional gel for mass spectrometric analyses. The spots were digested with trypsin and analyzed by MALDI mass spectrometry. Data base searching resulted in the identification of several 14-3-3 family proteins. The LAF389-induced spot gave the best fit to human 14-3-3 γ .

The LAF389-inducible Form of 14-3-3 γ Lacks N-terminal Processing—Upon close inspection of the MALDI mass spectra of tryptic digests of the induced and constitutive forms of 14-

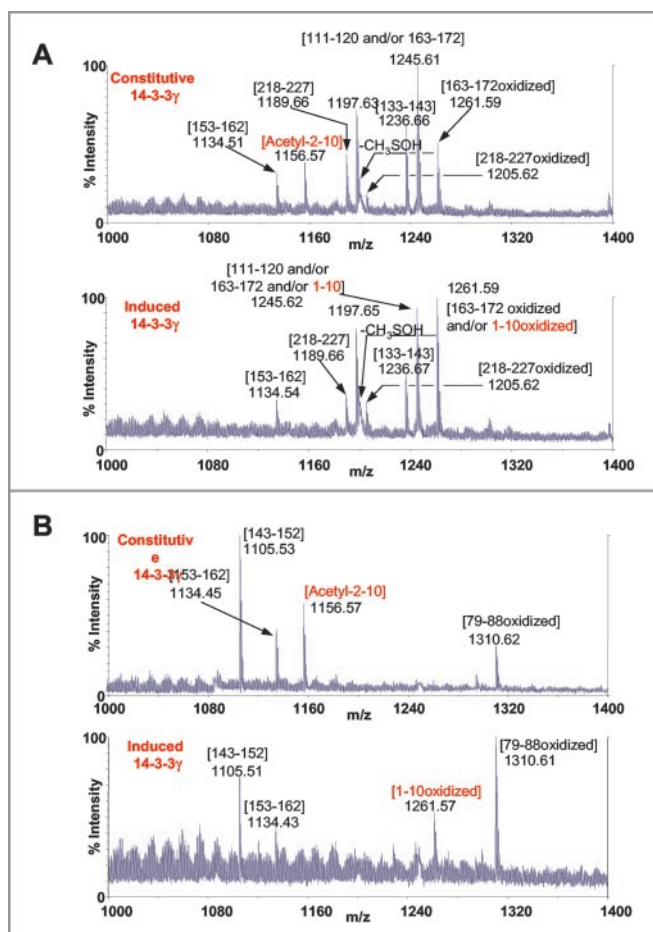


FIG. 3. MALDI-MS identification of an unprocessed 14-3-3 γ isoform. *A*, lysates of H1299 cells treated with LAF389 (200 nM, 24 h) were separated by two-dimensional gel electrophoresis, and spots were selected corresponding to the constitutive and induced forms of 14-3-3 γ . Spots were digested with trypsin and analyzed by MALDI-MS as described under “Experimental Procedures.” Note the presence of a peak at 1156.5762 matching an N-acetylated N-terminal peptide (*Acetyl-2-10*) in the constitutive 14-3-3 γ form only. *B*, samples were prepared as in Fig. 2*A* but were digested with endoproteinase Lys-C. Note the unique peak at 1261.57 in the spectrum of the induced 14-3-3 γ form matching an unprocessed N-terminal peptide M(oxi)VDREQLVQK and a unique peak at 1156.57 in the spectrum of the constitutive form corresponding to the acetylated N-terminal peptide VDREQLVQK.

3-3 γ , a unique peak at m/z 1156.57 could be seen in the spectrum of the constitutive form that was absent in the spectrum of the induced form (Fig. 3*A*). This mass matched that calculated for $[M+H]^+$ of the acetylated N-terminal peptide VDREQLVQK (amino acids 2–10). In the spectrum of the induced form, no mass was detected that fit this sequence with or without N-terminal acetylation. Instead, in both spectra, peaks at m/z 1245.61 and 1261.59 were observed. Three tryptic peptides of 14-3-3 γ had masses matching m/z 1245.61: peptides (111–120) ($[M+H]^+ = 1245.51$ Da), (163–172) ($[M+H]^+ = 1245.62$ Da), and (1–10) ($[M+H]^+ = 1245.66$ Da). Therefore, assignment based solely on mass was not possible. The peak at m/z 1261.59 matched perfectly the mass of the N-terminal tryptic peptide (1–10) M(oxi)VDREQLVQK, $[M+H]^+ = 1261.65$ Da) if its methionine was considered as oxidized (as revealed by the metastable loss of CH_3SOH). Coincidentally, a second peptide which also contained an oxidized methionine (163–172, EHM(oxi)QPTHPIR, $[M+H]^+ = 1261.61$ Da) perfectly matched that molecular mass as well.

Interestingly, relative to a reference peak at m/z 1197.63, the intensity of the peak at m/z 1261.59 was lower in the spectrum

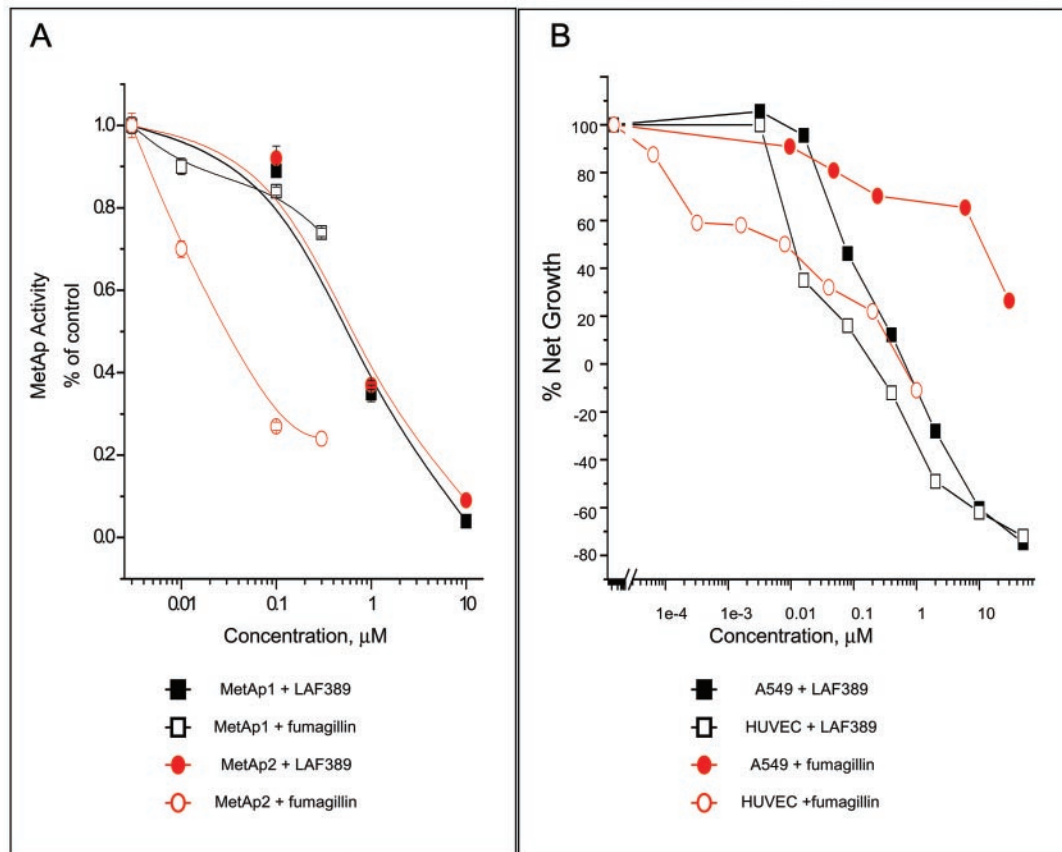


FIG. 4. **Inhibition of MetAp enzymatic and antiproliferative activities by LAF389 and comparison with fumagillin.** *A*, effects on cleavage of methionine from the tripeptide Met-Ala-Ser by recombinant purified human MetAp types I and II. *B*, effects on proliferation of A549 lung epithelial tumor cells and endothelial cells (*HUVEC*). Cell proliferation in response to LAF389 and fumagillin was measured after a 72-h exposure to compound. Data are presented as changes relative to cell density at the time of compound addition; positive % net growth indicates an increase in cell number relative to initial cell density, and negative % net growth indicates a decrease in cell number relative to initial cell density.

of the constitutive isoform *versus* that of the induced isoform. This result suggested that the peak at m/z 1261.59 possibly corresponded to a mixture of two peptides in the induced form, whereas that peak would have been generated by a single peptide (163–172) in the constitutive form. This possibility was confirmed by MALDI-MS analysis of endoproteinase Lys-C digests of the inducible and constitutive isoforms of 14-3-3 γ (Fig. 3B). The MALDI spectrum showed that the peak at m/z 1261.57 (matching the unprocessed N-terminal peptide M(oxi)VDREQLVQK) was found only in the spectrum of the induced 14-3-3 γ form, whereas the peak at m/z 1156.57 (matching the acetylated N-terminal peptide VDREQLVQK) was found only in the constitutive form (Fig. 3B). The combined data from both MS methods (Lys-C and trypsin digest) resulted in sequence coverage of 94 and 82% for the constitutive and induced forms of 14-3-3 γ , respectively. Confirmation of the assignment of the N-terminal sequences was performed by nano-ESMS/MS sequencing. Direct selection of the triply charged parent ion at m/z 421.22 from the Lys-C digest of the induced 14-3-3 γ isoform and subsequent fragmentation produced sufficient y and b type fragment ions to identify unambiguously the sequence of the peptide as M(oxi)-VDREQLVQK (1–10). A similar analysis of the amino-terminal peptide of the tryptic digest of the constitutive 14-3-3 γ confirmed the complete sequence as acetyl-VDREQLVQK (2–10) (data not shown). The lack of acetylation in the inducible isoform readily explained the focusing position at a higher pH relative to the constitutive isoform.

LAF389 Inhibits Methionine Aminopeptidases Directly—The retention of the initiator methionine in the inducible 14-3-3 γ isoform suggested LAF389 treatment of cells reduced MetAp activity, but the data could not distinguish between a direct effect of LAF389 on MetAp activity *versus* LAF389 effects on proteins that regulated MetAp activity. To address this question, both human MetAp isoforms were expressed in recombinant form and tested in an enzymatic assay using a methionine-containing peptide as substrate (Fig. 4A). Both MetAp1 and 2 were inhibited by LAF389, thus establishing MetAps as direct targets of LAF389. Fumagillin, a well known covalently reacting inhibitor specific for MetAp2 (20, 21), was tested in parallel in these assays. For MetAp2, the IC_{50} of LAF389 was 800 nM in this assay format, compared with 30 nM for fumagillin. In contrast to LAF389, however, fumagillin caused at most 20% inhibition of MetAp1 even at 300 nM.

LAF389 Has Pronounced Activity on Endothelial Cells—Fumagillin selectively inhibits endothelial cell proliferation, and structure-activity relation studies of fumagillin analogues have shown that its anti-proliferative effect correlates well with MetAp2 enzyme inhibition (21, 22). Therefore, it was of interest to test whether LAF389 could inhibit endothelial cell proliferation. In monolayer growth assays, LAF389 was a potent inhibitor of HUVEC proliferation, with a 20 nM IC_{50} , roughly 10-fold more potent than on A549 tumor epithelial cells (Fig 4B). The endothelial specificity of LAF389 was less pronounced than that seen with fumagillin, which had ~1000-fold selectivity for endothelial growth inhibition. LAF389 also differed from fumagillin in that substantial cell death of A549

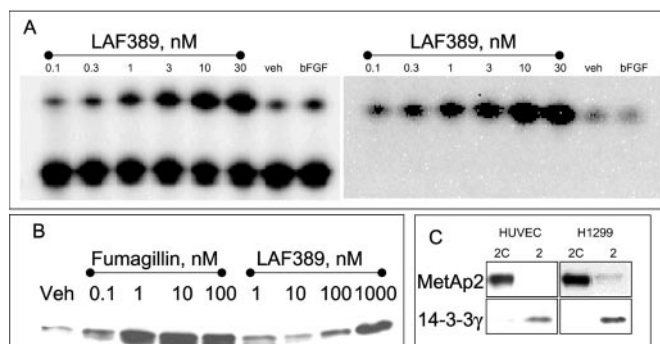


FIG. 5. Effects of MetAp inhibition or siRNA suppression on processing of 14-3-3 γ . *A*, IEF-immunoblotting analysis of HUVEC exposed to LAF389 at the indicated concentrations for 18 h. Cell lysates were probed with a polyclonal 14-3-3 γ specific antibody (*left*) or with a monoclonal antibody specific for the unprocessed, MetVal, form of 14-3-3 γ (*right*). *B*, SDS-PAGE Western blot analysis of HUVEC exposed to LAF389 or fumagillin at the indicated concentrations for 18 h. The membrane was probed with a monoclonal antibody specific for the unprocessed form of 14-3-3 γ . *C*, SDS-PAGE Western blots of cells were treated with siRNA specific for MetAp2 or with a control mismatch siRNA as indicated under “Experimental Procedures.” Cell lysates were resolved by SDS-PAGE, transferred to nitrocellulose, and probed with an antibody specific for MetAp2 (*top*) or the monoclonal antibody specific for unprocessed 14-3-3 γ .

cells was seen at micromolar concentrations of LAF389, whereas even at 10 μ M, fumagillin was only cytostatic for this carcinoma cell line.

MetAp processing of 14-3-3 γ was inhibited in endothelial cells treated with LAF389, as detected by IEF-Western blotting using a polyclonal antibody to the γ isoform (Fig. 5*A*, *left*). The unprocessed form of 14-3-3 γ could also be detected with a monoclonal antibody raised against a 15-amino acid peptide from the amino terminus of 14-3-3 γ (Fig. 5*A*, *right*). This monoclonal antibody permitted detection of the unprocessed form of 14-3-3 γ in Western blots of lysates resolved on conventional SDS-PAGE gels. Treatment of endothelial cells with either LAF389 or fumagillin caused the appearance of the unprocessed form of 14-3-3 γ , with the maximal response to fumagillin at 1 nM and maximal response to LAF389 at 1 μ M (Fig. 5*B*).

Unprocessed 14-3-3 γ could also be detected in cells treated with siRNA to lower the level of MetAp2 (Fig. 5*C*). The level of MetAp2 was reduced \sim 75% by this treatment. Both endothelial cells and tumor epithelial cells had detectable levels of the unprocessed form of 14-3-3 γ upon treatment with MetAp2 siRNA, suggesting that in both cell types, 14-3-3 γ may be processed at least in part by the MetAp2 isoform.

Crystal Structure of a MetAp2/bengamide Complex—To understand the mechanism of inhibition of methionine aminopeptidases by bengamides, we co-crystallized human MetAp2 with LAF153. LAF153 is the primary metabolite of LAF389 both in cells and *in vivo* and is an equally potent inhibitor of human MetAp2 *in vitro* (data not shown). The structure, refined at 1.6 Å resolution (Table II), reveals that LAF153 binds in a manner that closely mimics that expected for a polypeptide substrate. The MetAp2 active site is a deep invagination in the surface of the enzyme, with a dinuclear metal center that is critical for enzymatic activity (23). The innermost portion of the active-site cleft forms the P1 pocket, which recognizes the N-terminal methionine of a substrate polypeptide. The rather hydrophobic P1' pocket, which accommodates the penultimate residue, lies in the central portion of the cleft, whereas the P2' pocket is formed at its solvent-exposed surface. In the LAF153 inhibitor complex, the hydrophobic alkenyl linkage with attached *tert*-butyl alcohol substituent mimics the methionine side chain and

TABLE II
Data collection and refinement statistics

Data collection statistics	
Space group	C222 ₁
Cell parameters (Å)	$a = 90.61, b = 99.04, c = 101.38$
Resolution range ^a (Å)	50.0 – 1.6 (1.66 – 1.60)
Unique/total reflections	59,626/679,600
Redundancy	11.4
Completeness ^a (%)	98.8 (89.8)
$R_{\text{merge}}^{\text{a, b}}$ (%)	6.0 (45.0)
Refinement and model statistics	
R -factor/ $R_{\text{free}}^{\text{c}}$ (%)	20.4/21.1
Resolution range (Å)	50.0 – 1.6
Number of protein atoms	2,787
Number of inhibitor atoms	32 (LAF153: 27, <i>t</i> -BuOH: 5)
Number of water molecules/ Co ²⁺ ions	272/2
RMSD ^d bond lengths (Å)	0.009
RMSD bond angles (°)	1.40
Average B-value (Å ²)	
Main-chain/side-chain	20.5/23.1
LAF153/ <i>t</i> -BuOH/water/Co ²⁺	21.8/34.7/32.7/18.3

^a Values in the parentheses are for the reflections in the highest resolution shell (1.66 – 1.6 Å).

^b $R_{\text{merge}} = \sum_h \sum_i |I(h,i) - \langle I(h) \rangle| / \sum_h \sum_i I(h,i)$, where $I(h,i)$ is the intensity of the i th measurement of reflection h and $\langle I(h) \rangle$ is the average value over multiple measurements.

^c $R = \sum |F_o| - |F_c| / \sum |F_o|$, where R_{free} is calculated for 5% test set of reflections.

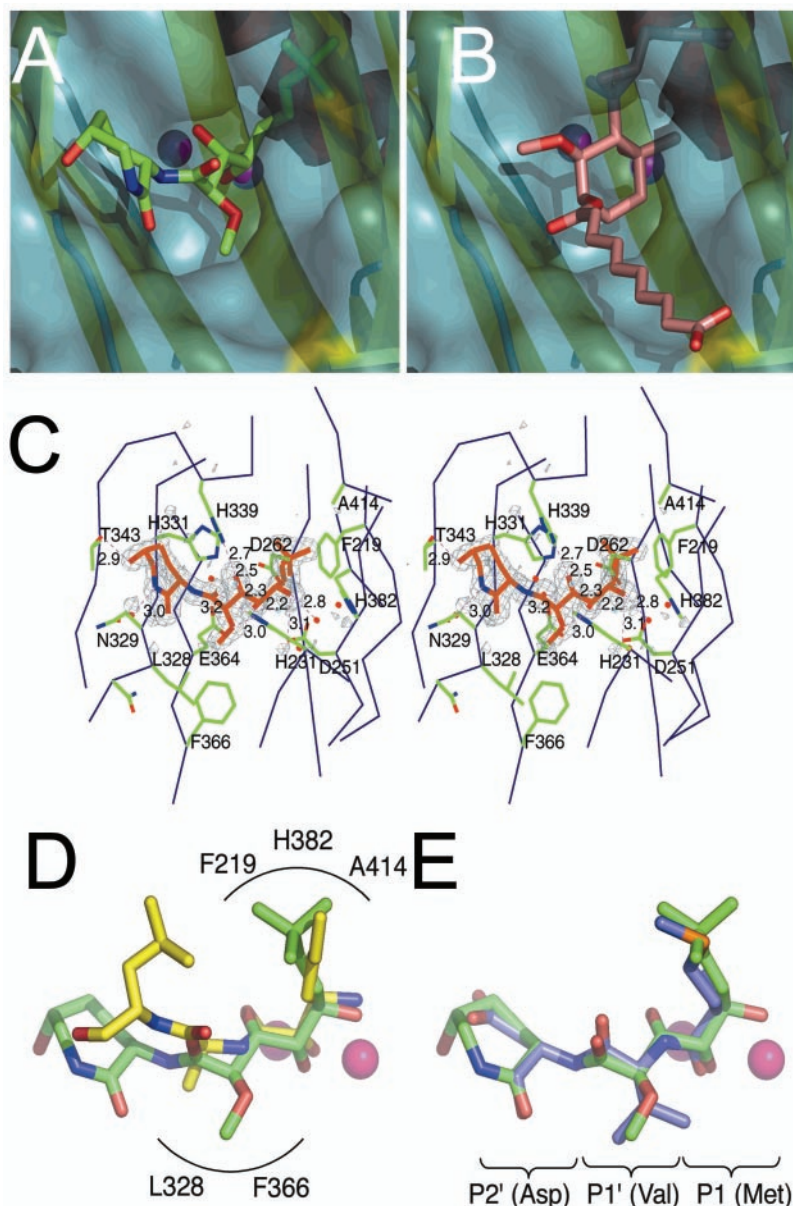
^d RMSD, root-mean-square deviation.

occupies the deeply buried P1 pocket, the hydroxymethyl moiety extends into the P1' pocket, and the caprolactam ring is coordinated in the solvent-exposed P2' region (Fig. 6*A*). The 3, 4, and 5 hydroxyl groups of the inhibitor coordinate the two active-site cobalt ions. As discussed below, the geometry of the interactions of the hydroxyl groups with the di-cobalt center is remarkably similar to that observed for the main chain amide and carbonyl groups of peptidic inhibitors of aminopeptidases (24).

The P1 pocket is formed largely by residues Phe-219, His-382, and Ala-414. The *t*-butyl group of LAF153 is in hydrophobic contact with each of these residues. The double bond through which the *t*-butyl group is attached is likely required for its proper positioning within this pocket. Interestingly, in the unliganded MetAp2 protein, which was crystallized in a buffer containing butanol (12), a butanol molecule is bound in the same position as that of the *t*-butyl group of LAF153. The smaller P1' pocket is formed by Leu-328, Phe-366, and His-231. The side chain imidazole of His-231 hydrogen bonds with the carbonyl group that is adjacent to the methoxy side chain. We expect that this portion of the inhibitor mimics the penultimate residue in a peptide substrate (Fig. 6*E*). The size and character of the P1' pocket is consistent with the requirement for small, uncharged amino acids in this position in protein substrates (23). In contrast, MetAps show little substrate specificity at the P2' position (the third residue in a substrate peptide). This region in MetAp2 is relatively open and solvent exposed; in the inhibitor complex, it is occupied by the lactam ring, which is coordinated by hydrogen bonds from Thr-343 and Asn-329 (through a bridging water molecule).

The observed mode of binding and inhibition for LAF153 is unrelated to that described previously for fumagillin (12) (Fig. 6*B*), but is very similar to that of a bestatin-derived inhibitor of *Escherichia coli* MetAp (24). Bestatin is a naturally occurring peptidic inhibitor of aminopeptidases (25) and has been modified to create an inhibitor specific for *E. coli* MetAp by altering amino acid side chains (24). Superposition of the present structure with the bestatin-based inhibitor (3*R*)-amino-(2*S*)-hydroxylheptanoyl-Ala-Leu-Val-Phe-OMe in complex with *E. coli* MetAp is shown in Fig. 5*D*. This non-hydrolyzable inhibitor

FIG. 6. Structure of human MetAp2 in complex with the bengamide analogue LAF153. *A*, the active-site cleft is represented as a semi-transparent surface. The bound LAF153 inhibitor is shown as a *stick model* with oxygen atoms colored *red*, nitrogen atoms *blue*, and carbon atoms *green*. The β -sheet secondary structure near the active site is represented as a *ribbon* under the surface. The two active-site cobalt ions are shown as *purple spheres*. The *t*-butyl group of LAF153 extends into the innermost portion of the cleft (the P1 pocket), whereas the lactam ring is coordinated in the shallow P2' pocket at the surface of the enzyme. Note also that the hydroxyl-oxygen atoms in the inhibitor coordinate the cobalt ions. This mode of binding is unrelated to that of fumagillin, which is shown in *panel B*. *B*, the structure of fumagillin in complex with human MetAp2. The orientation is the same as in *panel A*. Unlike LAF153, fumagillin makes only modest contact with the dinuclear metal center and instead forms a covalent bond with His-231. *C*, stereodiagram showing the details of the interactions of LAF153 in the active site. The $F_o - F_c$ omit electron density map calculated without the inhibitor is shown in *gray* and is contoured at 3.5σ . The cobalt ions are shown as *cyan spheres*, ordered water molecules as *red spheres*, and putative hydrogen bonds as *thin dashed lines*. *D*, superposition of LAF153 (*green*) with a bestatin-derived inhibitor (shown in *yellow*). Residues Phe-219, His-382, and Ala-414 form the hydrophobic P1 pocket, and Leu-328 and Phe-366 form the P1' pocket. Note the similarity in cobalt coordination and in the position of the norleucine side chain and *t*-butyl moiety of LAF153 in the P1 pocket (see text). *E*, 14-3-3 γ -derived tripeptide Met-Val-Asp is modeled onto the LAF153 structure. The tripeptide was manually fit to the structure and then energy-minimized. The superposition makes obvious the close steric correspondence between LAF153 (carbon atoms colored *green*) and the substrate peptide (with carbon atoms colored *violet*).



differs from a substrate peptide in two ways: (i) the N-terminal methionine is replaced by norleucine in a D rather than an L configuration; and (ii) the peptide backbone is extended by one atom between the first and second residues. The superposition reveals that the norleucine side chain extends into the space equivalent to that occupied by the *t*-butyl group in the LAF153 complex. Additionally, the comparison shows an essentially identical mode of metal coordination. The five-hydroxy group in LAF153 coordinates the first cobalt ion in a manner equivalent to that of the N-terminal amine group of the *E. coli* inhibitor. Likewise, the four-hydroxy group bridges between the two metals, and the three-hydroxy group coordinates the second cobalt in the same manner as the keto-oxygen in the bestatin-based inhibitor. The distances between the hydroxyl oxygens and the cobalt ions range from 2.2 to 2.5 Å in the LAF153 complex (Fig. 6C). Modeling of the three N-terminal residues of 14-3-3 γ on LAF153 shows the close steric correspondence between the various components of the inhibitor and the P1, P1', and P2' side chains of the substrate (Fig. 6E). We conclude that LAF153 and the related bengamide LAF389 are pseudo-substrate inhibitors of methionine aminopeptidases.

DISCUSSION

The data presented here demonstrate the utility of proteomics-based analysis to identify the mode of action of novel agents. Prior to this study, bengamides had been characterized as potent antiproliferative agents capable of inhibiting tumor cell growth *in vitro* and in animal tumor models. Attempts to identify possible mechanistic targets of bengamides by profiling in the NCI 60 cell line antiproliferative assay, as well as tests in a number of enzymatic assays, were unable to identify a molecular target of the compound class. Proteomic analysis was therefore undertaken to identify, in a non-target-biased manner, molecular changes in cellular proteins in response to bengamide treatment. Many changes were observed in cellular proteins, which could reflect either direct or indirect effects of bengamides on cell processes. By pursuing in detail the nature of the change in one of the proteins, 14-3-3 γ , the proteomic approach permitted eventual identification of an unanticipated molecular target of bengamides, methionine aminopeptidases.

Bengamides differ from the previously reported MetAp inhibitors, fumagillin and ovalicin, in several respects. Inhibition

by fumagillin and ovalicin is due to a covalent interaction between an epoxide group on the compound with the His-231 residue at the active site of MetAp2 (12). Fumagillin and ovalicin are also strikingly selective inhibitors of endothelial cell proliferation, whereas bengamides inhibit proliferation of all cell types tested, including both endothelial and epithelial cells. In lower organisms, viability requires at least one functional MetAp isoform (26); given that bengamides inhibit the only two known human isoforms of MetAps, their breadth of cytotoxic activity might have been predicted. However, despite the lack of specificity *in vitro*, tumor-specific activity was seen with bengamides *in vivo*, as demonstrated by the striking anti-tumor activity in xenograft models at well tolerated doses (3). In additional studies comparing more frequent dosing, LAF389 has been observed to result in tumor regression,² an effect more pronounced than the *in vivo* responses reported with a potent fumagillin analogue, TNP-470, which gave at most cytostatic activity in human tumor xenograft models (27).

Based on the available literature, it remains unclear why the anti-proliferative activity of fumagillin analogues is selective for endothelial cells, because both endothelial and epithelial cells express both known human MetAp isoforms, and because equivalent inhibition has been reported when MetAp2 is immunoprecipitated from endothelial or epithelial cells treated with a fumagillin analogue (28, 29). One possibility is that human MetAp isoforms process distinct sets of substrates, as has been suggested for the yeast isoforms (30), and that among the proteins processed by MetAp2, one or more is required for endothelial cell viability. Selective substrate processing by MetAp2 is suggested by the current data. siRNA depletion of MetAp2 protein was sufficient to block processing of 14-3-3 γ , suggesting that this protein might be preferentially processed by MetAp2 and may not be a substrate for MetAp1. Additional experiments are in progress to deplete cells of MetAp1 by using siRNA technology to see whether MetAp1-selective substrates can be detected. The current data, however, do not suggest that 14-3-3 γ processing changes are responsible for the endothelial selectivity of MetAp2 inhibitors, because processing of 14-3-3 γ is inhibited in both endothelial and epithelial cells treated with MetAp inhibitors. 14-3-3 γ processing changes are also unlikely to be responsible for the anti-proliferative effects of MetAp inhibitors. 14-3-3 proteins in general are reported to regulate numerous proteins involved in cell cycle progression and cell death. However, of the processes reported to be regulated by 14-3-3 isoforms, only a very few have been shown to be selective for the γ isoform, and changes in amino-terminal processing upon treatment with bengamides were not observed in 14-3-3 isoforms other than γ . Nevertheless, the observed change in 14-3-3 γ processing is the first report of an easily detectable cellular marker for pharmacological inhibition of MetAp activity, and this response has the potential to serve as a biomarker for *in vivo* responses to MetAp inhibition.

Cells treated with bengamides clearly express multiple changes at the protein level, in addition to the characterized changes in 14-3-3 γ . Of the proteins with changes noted in Table I, to date only the change in 14-3-3 γ has been characterized. It is likely that the other proteins listed in Table I had alterations other than or in addition to amino-terminal processing, because both increases and decreases in pI were observed. Moreover, the list of proteins in Table I is by no means a complete catalogue of all cellular proteins altered by bengamide treatment. In experiments not shown, Edman degradation of total cell lysates from bengamide-treated *versus* control cells showed

that bengamide treatment caused a 20% increase in N-terminal methionine residues. The consequences of retaining an N-terminal methionine may include changes in protein stability upon retention of N-terminal methionine, as has been demonstrated in a yeast model system (30), that are suggested to be mediated by alterations in rates of proteasome degradation (31). Retention of N-terminal methionine also prevents N-terminal myristoylation and causes mislocalization of proteins within cells, as has been reported for endothelial nitric oxide synthase in response to treatment with TNP-470 (32). A more complete identification of MetAp substrates, *e.g.* by two-dimensional electrophoresis, remains a technical challenge. Cleavage of N-terminal methionine from a protein causes a minimal change in molecular weight and is not expected to lead to large changes of isoelectric points unless accompanied by acetylation or other post-translational processing such as myristoylation of the newly exposed amino group. This possibility may explain why so few changes were observed in the current study, as well as in earlier reports (29).

Another hypothesis connecting MetAp inhibition to cell cycle arrest and cell death is that MetAp inhibition alters the association between MetAps and other proteins. Two proteins have been reported recently to associate with MetAp2: flotillin (33) and the metastasis-associated protein S100A4 (34). No functional consequences for cell growth were shown for these associated proteins. In contrast, MetAp2 association with eIF2 α has been reported to safeguard protein translation (35, 36). MetAp2 binding to eIF2 α is reported to protect eIF2 α from phosphorylation, a modification that stabilizes the eIF2 α / β / γ -GDP-eIF2B complex and prevents the turnover of eIF2B. MetAp2 binding to eIF2 α is also reportedly regulated by O-linked glycosylation and phosphorylation (37). Whether these particular post-translational modifications of MetAp2 and eIF2 α are bengamide-responsive is not yet known, but it is of interest that in the initial proteome analysis, the isoelectric points of both MetAp2 and eIF2 α were affected by bengamide treatment. Additional experiments are in progress to identify the nature of the changes in MetAp2 and eIF2 α and to test whether these changes mediate the antiproliferative effects of bengamides as well as fumagillin.

REFERENCES

1. Quiñoà, E., Adamczeski, M., Crews, P., and Bakus, G. J. (1986) *J. Org. Chem.* **51**, 4494–4497
2. Thale, Z., Kinder, F. R., Bair, K. W., Bontempo, J., Czuchta, A. M., Versace, R. W., Phillips, P. E., Sanders, M. L., Wattanasin, S., and Crews, P. (2001) *J. Org. Chem.* **66**, 1733–1741
3. Kinder, F. R., Versace, R. W., Bair, K. B., Bontempo, J. M., Cesarz, D., Chen, S., Crews, P., Czuchta, A. M., Jagoe, C. T., Mou, Y., Nemzek, R., Phillips, P. E., Tran, L. D., Wang, R. M., Weltchek, S., and Zabludoff, S. (2001) *J. Med. Chem.* **44**, 3692–3699
4. Li, X., and Chang, Y.-H. (1995) *Biochim. Biophys. Acta* **1260**, 333–336
5. Li, X., and Chang, Y.-H. (1996) *Biochem. Biophys. Res. Commun.* **227**, 152–159
6. Nagase, T., Miyajima, N., Tanaka, A., Sazuka, T., Seki, N., Sato, S., Tabata, S., Ishikawa, K., Kawarabayashi, Y., Kotani, H., and Nomura, N. (1995) *DNA Res.* **2**, 37–43
7. Kinder, F. R., Jr., Wattanasin, S., Versace, R. W., Bair, K. W., Bontempo, J., Green, M. A., Lu, Y. J., Marepalli, H. R., Phillips, P. E., Roche, D., Tran, L. D., Wang, R. M., Waykole, L., Xu, D. D., and Zabludoff, S. (2001) *J. Org. Chem.* **66**, 2118–2122
8. Rabilloud, T., Adessi, C., Giraudel, A., and Lunardi, J. (1997) *Electrophoresis* **18**, 307–316
9. Towbin, H., Özbey, Ö., and Zingel, O. (2001) *Electrophoresis* **22**, 1887–1893
10. Mueller, D. R., Schindler, P., Coulot, M., Voshol, H., and van Oostrum, J. (1999) *J. Mass Spectrom.* **34**, 336–345
11. Elbashir, S. M., Harborth, J., Lendeckel, W., Yalcin, A., Weber, K., and Tuschl, T. (2001) *Nature* **411**, 494–498
12. Liu, S., Widom, J., Kemp, C. W., Crews, C. M., and Clardy, J. (1998) *Science* **282**, 1324–1327
13. Otwinowski, Z., and Minor, W. (1997) *Methods Enzymol.* **276**, Part A, 307–326
14. Jones, T. A., and Kjeldgaard, M. (1997) *Methods Enzymol.* **277**, 173–208
15. Brunger, A. T., Adams, P. D., Clore, G. M., DeLano, W. L., Gros, P., Grosse-Kunstleve, R. W., Jiang, J. S., Kuszewski, J., Nilges, M., Pannu, N. S., Read, R. J., Rice, L. M., Simonson, T., and Warren, G. L. (1998) *Acta Crystallogr. Sect. D Biol. Crystallogr.* **54**, 905–921
16. Tzivion, G., Shen, Y. H., and Zhu, J. (2001) *Oncogene* **20**, 6331–6338
17. Megidish, T., Cooper, J., Zhang, L., Fu, H., and Hakamori, S. (1998) *J. Biol.*

² P. E. Phillips, F. R. Kinder, R. W. Versace, and J. Bontempo, unpublished data.

- Chem.* **273**, 21834–21845
18. Dubois, T., Rommel, C., Howell, S., Steinhussen, U., Soneji, Y., Morrice, N., Moelling, K., and Aitken, A. (1997) *J. Biol. Chem.* **272**, 28882–28888
 19. Martin, H., Patel, Y., Jones, D., Howell, S., Robinson, K., and Aitken, A. (1993) *FEBS Lett.* **331**, 296–303
 20. Sin, N., Meng, L., Wang, M. Q. W., Wen, J. J., Bornmann, W. G., and Crews, C. M. (1997) *Proc. Natl. Acad. Sci. U. S. A.* **94**, 6099–6103
 21. Griffith, E. C., Su, Z., Turk, B. E., Chen, S., Chang, Y.-H., Wu, Z., Biemann, K., and Liu, J. O. (1997) *Chem. Biol.* **4**, 461–471
 22. Griffith, E. C., Su, Z., Niwayama, S., Ramsay, C. A., Chang, Y.-H., and Liu, J. O. (1998) *Proc. Natl. Acad. Sci. U. S. A.* **95**, 15183–15188
 23. Lowther, W. T., and Matthews, B. W. (2000) *Biochim. Biophys. Acta* **1477**, 157–167
 24. Lowther, W. T., Orville, A. M., Madden, D. T., Lim, S., Rich, D. H., and Matthews, B. W. (1999) *Biochemistry* **38**, 7678–7688
 25. Suda, H., Aoyagi, T., Takeuchi, T., and Umezawa, H. (1976) *Arch. Biochem. Biophys.* **177**, 196–200
 26. Li, X., and Chang, Y.-H. (1995) *Proc. Natl. Acad. Sci. U. S. A.* **92**, 12357–12361
 27. Ingber, D., Fujita, T., Kishimoto, S., Sudo, K., Kanamaru, T., Brem, H., and Folkman, J. (1990) *Nature* **348**, 555–557
 28. Wang, J., Lou, P., and Henkin, J. (2000) *J. Cell. Biochem.* **77**, 465–473
 29. Turk, B. E., Griffith, E. C., Wolf, S., Biemann, K., Chang, Y. H., and Liu, J. O. (1999) *Chem. Biol.* **6**, 823–833
 30. Chen, S., Vetro, J. A., and Chang, Y.-H. (2002) *Arch. Biochem. Biophys.* **398**, 87–93
 31. Varshavsky, A. (1996) *Proc. Natl. Acad. Sci. U. S. A.* **93**, 12142–12149
 32. Yoshida, T., Kaneko, Y., Tsukamoto, A., Han, K., Ichinose, M., and Kimura, S. (1998) *Cancer Res.* **58**, 3751–3756
 33. Liu, W. F., and Liu, J. (2001) *Sheng Wu Hua Xue Yu Sheng Wu Wu Li Xue Bao (Shanghai)* **33**, 719–722
 34. Endo, H., Takenaga, K., Kanno, T., Satoh, H., and Mori, S. (2002) *J. Biol. Chem.* **277**, 26396–26402
 35. Wu, S., Gupta, S., Chatterjee, N., Hileman, R. E., Kinzy, T. G., Denslow, N. D., Merrick, W. C., Chakrabarti, D., Osterman, J. C., and Gupta, N. K. (1993) *J. Biol. Chem.* **268**, 10796–10801
 36. Datta, B., Chakrabarti, D., Roy, A., and Gupta, N. K. (1988) *Proc. Natl. Acad. Sci. U. S. A.* **85**, 3324–3328
 37. Datta, B., Ray, M. K., Chakrabarti, D., Wylie, D. E., and Gupta, N. K. (1989) *J. Biol. Chem.* **264**, 20620–20624

Proteomics-based Target Identification: BENGAMIDES AS A NEW CLASS OF METHIONINE AMINOPEPTIDASE INHIBITORS

Harry Towbin, Kenneth W. Bair, James A. DeCaprio, Michael J. Eck, Sunkyu Kim, Frederick R. Kinder, Anthony Morollo, Dieter R. Mueller, Patrick Schindler, Hyun Kyu Song, Jan van Oostrum, Richard W. Versace, Hans Voshol, Jeanette Wood, Sonya Zabudoff and Penny E. Phillips

J. Biol. Chem. 2003, 278:52964-52971.

doi: 10.1074/jbc.M309039200 originally published online October 8, 2003

Access the most updated version of this article at doi: [10.1074/jbc.M309039200](https://doi.org/10.1074/jbc.M309039200)

Alerts:

- [When this article is cited](#)
- [When a correction for this article is posted](#)

[Click here](#) to choose from all of JBC's e-mail alerts

This article cites 37 references, 12 of which can be accessed free at <http://www.jbc.org/content/278/52/52964.full.html#ref-list-1>